Synthesis, molecular docking and QSAR studies of 2, 4-disubstituted thiazoles as antimicrobial agents

Preeti Arora[1], Rakesh Narang[1*], Sonam Bhatia[1], Surendra Kumar Nayak[1], Sachin Kumar Singh[1], Balasubramanian Narasimhan[2]

[1]Department of Pharmaceutical Chemistry, School of Pharmaceutical Sciences, Lovely Professional University, Phagwara-144401, India.
[2]Faculty of Pharmaceutical Sciences, Maharshi Dayanand University, Rohtak-124001, India.

ABSTRACT

In present study a series of 2,4-disubstituted thiazole derivatives was synthesized and evaluated for their *in vitro* antibacterial and antifungal activities against *B. subtilis, E. coli, S. aureus, C. albicans* and *A. niger* by tube dilution method. The analysis of antimicrobial activity results indicated that the presence of NO_2 and OCH_3 groups at *para* position of phenyl group improved the antimicrobial activity significantly. Molecular docking studies also supported *in vitro* activity results and showed that NO_2 and OCH_3 groups containing compounds have greater affinity towards the target glucosamine-6-phosphate synthase. QSAR studies indicated that molecular connectivity index ($^2\chi^v$) and Kier's shape index ($\kappa\alpha_3$) are the key parameters for antimicrobial activity of synthesized thiazole derivatives and can be cosidered as important factors for interaction with target site of different microorganisms. It is pertinent to note that multi-target QSAR models were more effectual in demonstrating the antimicrobial activity than one-target QSAR models.

INTRODUCTION

The treatment of infectious diseases caused by bacteria, parasites, viruses and fungi always remains a global health problem because of increasing number of multi-drug resistant pathogenic microbial strains (Narang *et al*., 2012). Despite the availability of large number of antibiotics for clinical use, the emergence of antibiotic resistance in recent years against Gram-positive and Gram-negative bacterial and fungal strains constitutes an urgent need for the discovery of new class of antimicrobial agents (Perez *et al.*, 2014; Narasimhan *et al.*, 2009). Various sulfur and/or nitrogen containing heterocyclics belonging to the class of alkaloids, vitamins, pigments etc. possessing biological activities are reported in the literature (Ozdemir *et al.*, 2007). 1,3-thiazoles and their derivatives are important class of five membered heterocyclic compounds having sulphur and nitrogen at position-1 and -3, respectively.

1,3-thiazoles derivatives have been reported to possess wide range of biological activities like antibacterial (Bharti *et al.*, 2010), antifungal (Bharti *et al.*, 2010), antiviral (El-Sabbagh *et al.*, 2009), anti-inflammatory (Helal *et al.*, 2013), anticancer (Soares *et al.*, 2013), antitubercular (Mjambili *et al.*, 2014), antiplasmodial (Mjambili *et al.*, 2014), antiallergic (Ban *et al.*, 1998), anti-inflammatory (Ben *et al.*, 1998), antipsychotropic (Zablotskaya *et al.*, 2013), antiarthritic (Nishikaku *et al.*, 1993) etc. 1,3-thiazole nucleus is commonly found in the chemical structures of antiparasitic agents *viz.* nitazoxanide, aminitrozole and tenonitrozole (Cohen *et al.*, 2012). Morover, penicillin derivatives (antibacterial) (Ye *et al.*, 2013), vitamin B_1 (thiamine) (Wei *et al.*, 2014), bleomycin (Rahmutulla *et al.*, 2014) and tiazofurin (antineoplastic) (Popsavin *et al.*, 2006), ritonavir (anti-HIV) (Sevrioukova *et al.*, 2013), fanetizole (Styrt *et al.*, 1985) and meloxicam (anti-inflammatory) (Novakova *et al.*, 2014), nizatidine (antiulcer) (Jain *et al.*, 2014) are also thiazole ring containing important biologically active agents. Structure activity relationship study of thiazole based drugs/leads revealed that substituents on a particular position specifically at position 2 and 4 of the 1,3-thiazole ring affect the biological outcomes to a great extent.

* *Corresponding Author*
Rakesh Narang, Department of Pharmaceutical Chemistry, School of Pharmaceutical Sciences, Lovely Professional University, Phagwara-144401, India. Email: rakesh_nrng@yahoo.co.in

Molecular docking is a computer-assisted drug design (CADD) method used to predict the favourable orientation of a ligand (*viz.* drug) to a target (*viz.* receptor) when bound to each other to form a stable complex. By understanding of the favoured orientation in turn can be used to find out the strength of binding affinity between ligand and target site, *e.g.* by docking score (Sarojini *et al.*, 2010). Moreover, docking study can be used to find out type of interactions between ligand and receptor *viz.* hydrogen bonding and hydrophobic interactions.

Hence, molecular docking can be considered as first-line technique for a pharmaceutical lead discovery (Shoichet *et al.*, 2002). Moreover, *in silico* studies on 2,5-dichloro thienyl substituted thiazole derivatives carried out by the research group of Sarojini and co-workers (2010) have found that thiazole based analogues have potential to bind with the enzyme, L-glutamine: D-fructose -6 -phosphate amidotransferase.

This enzyme is commonly known by the trivial name of glucosamine-6-phosphate synthase (EC 2.6.1.16), which is characterized as a new antifungal target (Chmara *et al.*, 1984; Chmara *et al.*, 1986, Milewski *et al.*, 1988). This enzyme carries out transferase reaction which involves the transfer of ammonia group from L-glutamine to fructose-6-phosphate (Fru-6-P), which is followed by isomerisation of fructosamine-6-phosphate to glucosamine-6-phosphate (Dutka-Malen *et al.*, 1988; Bates *et al.*, 1966).

This reaction is involved in the formation of uridine diphosphate N-acetylglucosamine (UDP-GlcNAc), a product that is present in all class of organisms, but in case of fungi and bacteria it is solely used to build macromolecules related with cell wall assembly, *e.g.* chitins and mannoproteins in case of fungi and peptidoglycan in bacteria. Hence, the target glucosamine-6-phosphate synthase was selected for performing the *in silico* studies in present study. Quantitative structure–activity relationship (QSAR) is a significant part of chemometrics used to correlate experimentally determined biological activities with structural descriptors of chemical compounds (Hansch *et al.*, 1964).

The derived QSAR model can be further utilized to predict biological activity of compound not synthesized in the laboratory (Narang *et al.*, 2013). In light of above facts and in continuation of our research program focused on design and synthesis of novel antimicrobial agents an attempt has been made to synthesize 2,4-disubstituted thiazole derivatives and screened them for *in vitro* antibacterial and antifungal activities (Narang *et al.*, 2013; Narang *et al.*, 2012; Narang *et al.*, 2011; Kumar *et al.*, 2010; Kumar *et al.*, 2009). Further, to evaluate the active site interaction made by the synthesized compounds, molecular docking studies were carried out which is followed by 2D -QSAR studies to estimate the key descriptors that govern the anti-microbial activity of the compounds under investigation.

MATERIAL AND METHODS
Experimental

Melting points of synthesized compounds were determined in open glass capillaries on a sonar melting point apparatus and are uncorrected. Reaction progress was monitored by thin layer chromatography on silica gel sheets (Merck silica gel–G). [1]H Nuclear magnetic resonance (^{1}H NMR) spectra were recorded on Bruker Avance II 400 NMR spectrometer (400 MHz) at 298 K, in appropriate deuterated dimethyl sulfoxide. Chemical shifts were reported as δ (ppm) relative to tetramethylsilane (TMS) as internal standard. Infrared (IR) spectra were recorded as KBr pellet on Perkin Elmer FTIR spectrometer. The wave number is given in cm^{-1}.

General procedure for synthesis of 2-amino-4-phenylthiazole derivatives (3-12, Scheme 1 and 2)
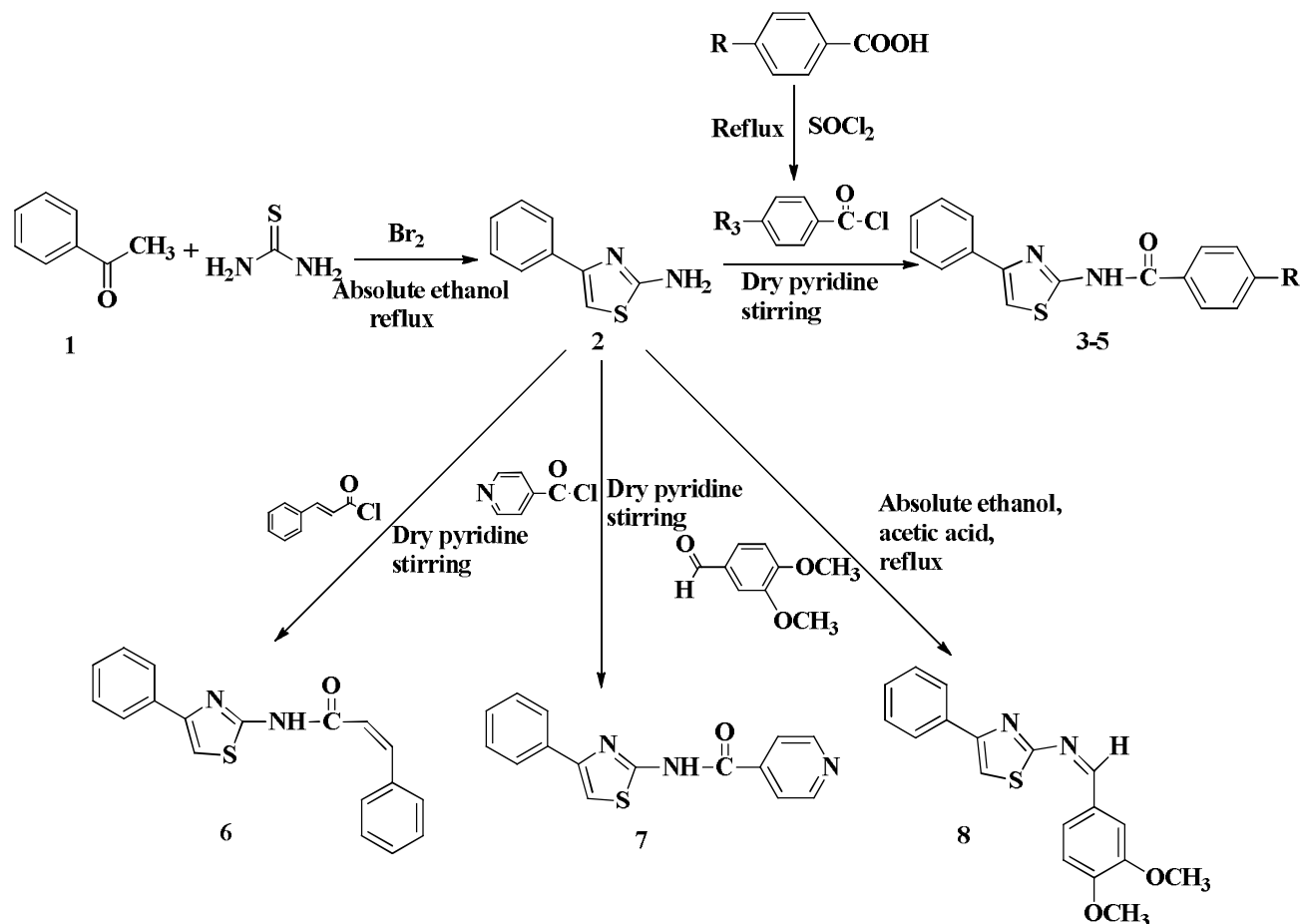#### *Synthesis of 2-amino-4-phenylthiazole (2, 10)*

To a mixture of acetophenone/*p*-nitroacetophenone (0.1 mol) and thiourea (0.2 mol) in absolute ethanol, bromine (0.2 mol) was added dropwise. After complete addition of bromine, reaction mixture was refluxed on a water-bath for 24 hrs. Then water was added to reaction mixture and heated until most of the solid was dissolved. The reaction mixture was filtered while hot. The filtrate was cooled and made alkaline using 20% ammonium hydroxide to obtain corresponding crude precipitate of 2-amino-4-phenylthiazole derivatives (**2** and **10**). Recrystallization from ethanol yielded the corresponding required product.

Synthesis of N-(4-phenyl-thiazol-2-yl)-benzamide/amide derivatives (3-7 and 11-12)

Acid chloride was prepared by refluxing corresponding acid (0.01 mol) with distilled thionyl chloride (0.178 mol) for 3-4 hrs. Excess of thionyl chloride was removed by distillation and synthesized acid chloride was used immediately for next step. The solution of corresponding acid chloride (0.002 mol) was added dropwise into solution of 2-amino-4-phenylthiazole/4-(4-nitro-phenyl)-thiazol-2-ylamine, (**2/10**) (0.001 mol) in dry pyridine, and stirred the reaction mixture at 0-10 ºC for 4-5 h. The mixture was allowed to stand overnight at room temperature. The solid precipitates of *N*-(4-phenyl-thiazol-2-yl)-benzamide/amide derivatives (**3-7** and **11-12**) were obtained, filtered and washed successively using dilute hydrochloric acid, 10% sodium bicarbonate solution and water subsequently, to remove the residual reactants.

Synthesis of 3,4-dimethoxy-benzylidene-4-phenyl-thiazol-2-yl-amine (8)

A mixture of 2-amino-4-phenyl thiazole, **3** (0.001 mol) and veratraldehyde (0.001 mol) in absolute ethanol was refluxed in presence of 2-3 drops of acetic acid for 7 hrs. After cooling solid precipitates of (3,4-dimethoxy-benzylidene)-(4-phenyl-thiazol-2-yl)-amine was obtained and crude precipitates were recrystallized from ethanol.

Scheme. 1: Scheme for synthesis of *N*-(4-phenyl-thiazol-2-yl)-benzamide/amide derivatives and (3,4-dimethoxy-benzylidene)-(4-phenyl-thiazol-2-yl)-amine.
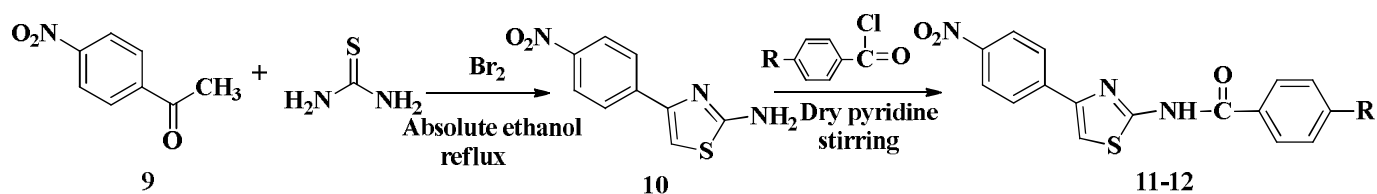
Scheme 2: Scheme for synthesis of 4-(4-nitro-phenyl)-thiazol-2-ylbenzamide derivatives.

Analytical data

2-Amino-4-phenylthiazole (2)

Yield (78%), Mp 138-141 °C; IR (KBr pellets, cm^{-1}): 3435, 3252 (NH str., primary amine), 3115 (CH str., aromatic), 1599 (C=N str.), 1440 (C=C str., aromatic), 651 (C-S str.); ^{1}H NMR (400 MHz, DMSO-d$_6$): δ 7.75-7.77 (d, 2H, C$_2$ and C$_6$ of phenyl ring), 7.30-7.34 (t, 2H, C$_3$ and C$_5$ of phenyl ring), 7.20-7.24 (t, 1H, C$_4$ of phenyl ring), 6.78 (s, 2H, NH$_2$), 6.75 (s, CH of thiazole nucleus).

N-(4-Phenyl-thiazol-2-yl)-benzamide (3)

Yield (71%), Mp 98-101 °C; IR (KBr pellets, cm^{-1}): 3362 (NH str., secondary amide), 3113 (CH str., aromatic), 1676 (C=N str.), 1611 (C=O str., secondary amide), 1442(C=C str., aromatic), 1305 (C-N str.,aromatic) 656 (C-S str.);^{1}H NMR

(400MHz,DMSO-d$_6$): δ 12.35 (s, 1H, NH), 8.16-8.18 (d, 2H, C$_2$ and C$_6$ of aromatic attach to C=O), 7.90-7.92 (d, 2H, C$_2$ and C$_6$ of phenyl ring attach to thiazole nucleus), 7.56-7.60 (t, 1H, C$_4'$ of aromatic attach to C=O), 7.48-7.52 (t, 2H, C$_3$ and C$_5$ of aromatic ring attach to C=O), 7.38-7.42 (t, 2H of C$_2$ and C$_5$ of phenyl ring attach to thiazole nucleus), 7.34-7.35 (s, 1H, CH of thiazole nucleus), 7.28-7.32 (t, 1H, C$_4$ of phenyl nucleus attach to thiazole nucleus).

4-Nitro-N-(4-phenyl-thiazol-2-yl)-benzamide (4)

Yield (73%), 169-172 °C; IR (KBr pellets, cm^{-1}): 3357 (NH str., secondary amide), 2923(CH str., aromatic), 1667 (C=O str., secondary amide), 1602 (C=N str.), 1550 (NO$_2$ str. asymmetric), 1470 (C=C str., aromatic), 1344 (C-N str., aromatic), 1327 (NO$_2$ str. symmetric) 654 (C-S str.); ^{1}H NMR (400 MHz,

DMSO-d_6): δ 12.39 (s, 1H, NH), 8.57-8.58 (d, 2H, C_3 and C_5 of NO_2 phenyl), 8.28-8.42 (m, 2H, C_2 and C_6 of NO_2 phenyl ring), 7.28-7.46 (m, 5H, phenyl ring attached to thiazole), 6.78-6.95 (s, 1H, CH of thiazole ring).

4-methoxy-N-(4-phenyl-thiazol-2-yl)-benzamide (5)

Yield (67.7%), Mp 163-166 °C; IR (KBr pellets, cm^{-1}): 3390 (NH str., secondary amide), 3112 (C-H str., aromatic), 2938 (CH str. of OCH_3), 1684 (C=O str., secondary amide), 1662 (C=N str.), 1605 (C=C str., aromatic), 1304 (C-N str.), 1256 (C-O-C str. asymmetric), 1129 (C-O-C str. symmetric), 658 (C-S str.); ^{1}H NMR (400 MHz, DMSO-d_6): δ 8.15-8.18 (d, 1H, C_2 of phenyl ring attached to thiazole nucleus), 7.90-7.94 (m, 3H, C_3, C_5 and C_6 of phenyl ring attached to thiazole nucleus), 7.39-7.42 (t, 1H, C_4 of phenyl ring attached to thiazole nucleus), 7.28-7.31 (s, 1H, CH of thiazole ring), 6.99-7.01 (d, 2H, C_2 and C_6 of methoxy phenyl ring), 6.90-6.93 (d, 2H, C_3 and C_5 of methoxy substituted phenyl ring), 4.88 (s, 1H, NH), 3.84-3.87 (s, 3H, OCH_3 attached to phenyl ring).

3-Phenyl-N-(4-phenylthiazol-2-yl)acrylamide (6)

Yield (68%), 174-177 °C; IR (KBr pellets, cm^{-1}): 3428 (NH str., secondary amide), 3142 (CH str., aromatic), 1675 (C=O str., secondary amide), 1622 (C=N str.), 1557 (C=C str., aromatic), 1493 (C=C str., aromatic), 1334 (C-N str., aromatic), 660 (C-S, str.); ^{1}H NMR (400 MHz, DMSO-d_6): δ 12.38 (s, 1H, NH), 7.87-7.89 (d, 2H, C_2 and C_6 of phenyl ring attached to thiazole), 7.54-7.58 (m, 3H, C_3, C_4 and C_5 of phenyl ring attached to thiazole), 7.39-7.47 (m, 5H, phenyl ring of cinnamoyl moiety), 7.37-7.38 (s, 2H, CH of CH=CH attached with phenyl nucleus), 6.95-6.98 (s, 1H, CH of thiazole).

N-(4-phenyl-thiazol-2-yl)-isonicotinamide (7)

Yield (55.1%), Mp 188-191 °C, IR (KBr pellets, cm^{-1}): 3433 (NH str., secondary amide), 3057 (CH str., aromatic), 1670 (C=O str., secondary amide), 1554 (C=N str.), 1423 (C=C str., aromatic), 1304 (C-N str., aromatic), 694 (C-S str.); ^{1}H NMR (400 MHz, DMSO-d_6): δ 9.192 (s, 1H, NH), 8.82-8.83 (d, 1H, C_3 of pyridine nucleus), 8.26-8.28 (d, 1H, C_4 of pyridine nucleus), 7.84-7.86 (d, 2H, C_2 and C_5 of pyridine nucleus), 7.38-7.52 (m, 5H of phenyl nucleus attached to thiazole nucleus).

(3,4-Dimethoxy-benzylidene)-(4-phenyl-thiazol-2-yl)-amine (8)

Yield (62.2%), Mp 224-227 °C, IR (KBr pellets, cm^{-1}): 2933 (CH str.), 1645 (C=N str.), 1599 (C=C str., aromatic), 1334 (C-N str), 1024 (C-O str.) 1250 (C-O-C str. asymmetric), 1130 (C-O-C str. symmetric) 653 (C-S str.); ^{1}H NMR (400 MHz, DMSO-d_6): δ 8.89 (s, 1H, CH of CH=N), 7.35-7.37 (d, 2H, C_1 and C_6 of aromatic ring attached to thiazole nucleus), 7.13-7.26 (t, 3H, C_3, C_4, C_5 of phenyl attached to thiazole nucleus), 6.76-7.05 (m, 3H, aromatic hydrogens of dimethoxy phenyl), 5.80 (s, 1H, CH of thiazole), 3.69-3.77 (s, 6H, OCH_3).

4-(4-Nitro-phenyl)-thiazol-2-ylamine (10)

Yield (55.4%), 221-224 °C, IR (KBr pellets, cm^{-1}): 3398, 3306 (NH str., primary amine), 3151 (CH str., aromatic), 1639 (C=N str.), 1593 (C=C str., aromatic), 1539 (NO_2 str., asymmetric), 1348 (NO_2 str., symmetric), 652 (C-S str.); ^{1}H NMR (400 MHz, DMSO-d_6): δ 6.82 (s, 2H, NH_2), 7.90-7.92 (d, 2H, C_2 and C_6 of phenyl ring), 8.52-8.57 (t, 2H, C_3 and C_5 of phenyl ring), 6.86 (s, 2H, NH_2), 6.80 (s, CH of thiazole nucleus).

N-[4-(4-Nitro-phenyl)-thiazol-2-yl]-benzamide (11)

Yield (60.9%), Mp 203-207 °C, IR (KBr pellets, cm^{-1}): 3400 (NH str., secondary amide), 3149 (CH str., aromatic), 1645 (C=O str., secondary amide), 1593 (C=C str., aromatic), 1558 (C=N str.), 1539 (NO_2 str. asymmetric), 1345 (NO_2 str., symmetric), 1338 (C-S str., aromatic); ^{1}H NMR (400 MHz, DMSO-d_6): δ 12.60 (s, 1H, NH), 8.65-7.80 (m, 4H, phenyl ring attached to thiazole nucleus), 7.20 (s, CH of thiazole) 7.02-6.90 (m, 5H, ArH)

4-Methoxy-N-[4-(4-nitro-phenyl)-thiazol-2-yl]-benzamide (12)

Yield (46.1%), Mp 198-201 °C, IR (KBr pellets, cm^{-1}): 3400 (NH str., secondary amide), 3149 (C-H str., aromatic), 2940 (CH str of OCH_3), 1645 (C=O str., secondary amide), 1593 (C=C str., aromatic), 1558 (C=N str.), 1539 (NO_2 str. asymmetric), 1338 (C-N str., aromatic), 1288 (C-O-C str. asymmetric), 1109 (C-O-C str. symmetric), 643 (C-S str.); ^{1}H NMR (400 MHz, DMSO-d_6): δ 12.58 (s, 1H, NH), 8.50-7.75 (m, 4H, phenyl ring attached to thiazole nucleus), 7.35-7.38 (s, CH of thiazole) 6.80-6.91 (m, 4H, ArH of methoxy phenyl ring), 3.87-3.90 (t, 3H, OCH_3 group attached to phenyl ring).

Antimicrobial evaluation

The antimicrobial estimation of synthesized compounds was carried out against Gram-positive bacteria: *Staphylococcus aureus MTCC 7443*, *Bacillus subtilis MTCC 441*, Gram-negative bacterium: *Escherichia coli MTCC 42* and fungal strains: *Candida albicans MTCC 183* and *Aspergillus niger MTCC 282* by tube dilution method (Cappucino and Sherman, 1999). The standard and test samples were dissolved in DMSO to give a concentration of 100 µg/ml. Dilutions of test and standard compounds were prepared in double strength nutrient broth – I.P. (bacteria) or Sabouraud dextrose broth I.P. (fungi) (Indian Pharmacopoeia, 2007). The samples were incubated at 37 °C for 24 h (bacteria), at 25 °C for 7 days (*A. niger*) and at 37 °C for 48 hrs (*C. albicans*) respectively, and the results were recorded in terms of MIC (the lowest concentration of compound inhibited the growth of microorganisms).

Molecular docking studies

Molecular docking studies of synthesized compounds were carried out on the target protein glucosamine-6-phosphate synthase (PDB Id: 1jxa) which catalysis the complex reaction involving ammonia transfer from L-glutamine to Fru-6-P, (Dutka-Malen *et al.*, 1988; Bates *et al.*, 1966) followed by isomerisation

of the formed fructosamine-6-phosphate to glucosamine-6-phosphate. The ligands were drawn in ChemBioDraw Ultra 12.0 followed by MM2 minimization of ligands (using ChemBio3D Ultra 12.0) by keeping a check on the connection error in the bonds. Protein and Grid preparation was done using Autodock Vina 1.1.2 (Trott *et al.*, 2010) and was used to perform molecular docking.

QSAR studies

The QSAR study was performed to correlate antimicrobial activity with physicochemical parameters of synthesized thiazole derivatives. The structures of synthesized thiazole derivatives were first pre-optimized with the Molecular Mechanics Force Field method (MM$^+$) included in Hyperchem 6.03 (1993) and the resulting geometries were further refined by means of the semiempirical method PM3 (parametric method-3). Gradient norm limit of 0.01 kcal/A° was utilized for the geometry optimization. TSAR 3.3 software for Windows (TSAR 3D Version 3.3, 2000) was used to calculate physicochemical parameters of lowest energy structures of synthesized thiazole derivatives. Further, the regression analysis was carried out using the SPSS software package (SPSS for Windows, 1999). The predictive powers of the developed models were supported by cross-validated r^2 (q^2) using leave one out (LOO) cross-validation method (Schaper, 1999). The statistical qualities of equations were further confirmed by the parameters like standard error of estimate (s), correlation coefficient (r), variance ratio (F) at specified degrees of freedom, root mean square error (RMSE) and predicted error sum of square (PRESS).

RESULTS AND DISCUSSION

Chemistry

The synthesis of the intermediate (**2** and **10**) and target compounds (**3-8** and **11-12**) were performed according to the reactions outlined in Scheme 1 and 2. Acid chloride was synthesized by refluxing acid with distilled thionyl chloride. Then, corresponding acid chlorides and synthesized thiazole derivatives were stirred at 0-10 °C in dry pyridine to yield the target *N*-(4-phenyl-thiazol-2-yl)-benzamide/amide derivatives (**3-7** and **11-12**). On the other hand, compound *N*-(3,4-dimethoxybenzylidene)-4-phenylthiazol-2-amine (**8**) was synthesized by condensation of intermediate (**2**) with veratraldehyde in presence of acetic acid. In this study we obtained some thiazole derivatives in good yield and some in moderate to low yield. The physicochemical properties of synthesized compounds are presented in Table 1.

Chemical structures of synthesized compounds (**2-8** and **10-12**) were ascertained on the basis of their ^{1}H NMR and IR spectral data. The appearance of singlet signal ranging from δ 6.75 to 7.38 ppm in the synthesized compounds confirmed the presence of CH of thiazole ring (compounds **2-8**). The presence of singlet signal of NH proton in compounds (**3-6** and **10-12**) in the range of δ 12.35-12.68 ppm revealed the formation of amide bond in the synthesized derivatives. The presence of aromatic protons in

synthesized derivatives was confirmed by the multiplet signal in the range of δ 7.01 to δ 8.65 ppm. The presence of methoxy group in compounds **5**, **8** and **12** was confirmed by singlet peak present in the region of δ 3.69-3.90 ppm. Moreover, the absence of singlet peak of NH$_2$ protons at δ 6.78 ppm in target compounds (**3-8** and **11-12**) and presence of same peak in intermediate (**2**) confirmed their synthesis.

The presence of the C=O functional group (compounds **3-7**, **11-12**) was indicated by the appearance of a stretching band around 1675 cm^{-1}, which is the characteristic of an amide linkage. The presence of the C=C str. (aromatic) was indicated by the appearance of a stretching band around 1450-1600 cm^{-1} in compounds **2-12**. The appearance of IR band around 3100-3400 cm^{-1} showed the presence of NH linkage of amide bond in synthesized derivatives. The appearance of C–S band around 650 cm^{-1} in compounds **2-12** indicated the presence of thiazole nucleus. In compounds **5**, **8** and **12** stretching band around 2940 cm^{-1} revealed the presence of methoxy group. Further, the aromatic nitro stretching around 1550 cm^{-1} (asymmetric NO$_2$ stretching) and 1350 cm^{-1} (symmetric NO$_2$ str.) depicted the presence of nitro functional group in synthesized compounds **4**, **11** and **12**. The presence of C-N bond in synthesized compounds was indicated by stretching band around 1334 cm^{-1}. In compounds **5**, **8** and **12** stretching at around 1130 cm^{-1} (symmetric C–O–C stretching) and 1250 cm^{-1} (asymmetric C–O–C stretching) revealed the presence of methoxy group.

Antimicrobial activity

The synthesized thiazole derivatives (**2-12**) were evaluated for their *in vitro* antibacterial activity against Gram-positive *S. aureus*, *B subtilis* and Gram-negative *E coli* and antifungal activity against *C. albicans* and *A. niger* by tube dilution method (Cappucino and Sherman, 1999). Double strength Nutrient broth I.P. and Sabouraud dextrose broth I.P. have been employed as media for growth of bacterial and fungal cells, respectively (Indian Pharmacopoeia, 2007).

The pMIC values of antimicrobial activity (μM ml^{-1}) are presented in Table 2. In case of *B. subtilis,* compounds **4**, **8**, **11** and **12** were found to be more active than the other synthesized derivatives with pMIC$_{bs}$ value range 3.92-4.01 μM ml^{-1}. Against *S. aureus*, compounds **4**, **8** and **12** were found to be most active than the other synthesized derivatives (pMIC$_{sa}$ range = 4.51-4.60 μM ml^{-1}). Again compounds **4**, **8** and **12** were found to be most potent against the Gram-negative bacteria, *E. coli* having pMIC$_{ec}$ value 4.51-4.60 μM ml^{-1} among synthesized derivatives.

On the other hand, results of antifungal activity revealed that the compounds **4**, **8**, **11** and **12** were able to produce good inhibitory activity against *C. albicans* (pMIC$_{ca}$ = 3.92-4.01 μM ml^{-1}). For antifungal activity against *A. niger* compounds **11** and **12** showed more potent activity having pMIC$_{an}$ value 4.01-4.23 μM ml^{-1} than other synthesized derivatives. Results of antimicrobial (antibacterial and antifungal) activities showed that compounds having phenyl substituted *p*-methoxy and *p*-nitro moieties were the most potent ones (pMIC range = 3.79-4.60 μM ml^{-1}) as compared

to other synthesized derivatives. Moreover, compounds with *p*-nitro phenyl moiety (**11** and **12**) attached at 4th position of thiazole ring were the most potent ones against tested antifungal strains (pMIC = 3.93-4.23 µM ml^{-1}). Further, it is observed that compound **12** having *p*-methoxy and *p*-nitro substituted phenyl ring showed most potent antimicrobial activity (pMIC = 4.60) among synthesized derivatives against *S. aureus* and *E. coli*.

Structure activity relationship on the basis of antimicrobial activity results

1. The replacement of hydrogen of NH_2 group (**2** and **10**) with benzamide (**3-5** and **11-12**), amide (**6-7**) and 3,4-dimethoxybenzylidene (**8**) led to a noticeable increase in antimicrobial activity of the synthesized compounds against *S. aureus* and *E. coli*. This may be due to the increase in lipophilicity of synthesized derivatives, which may allow them to easily penetrate the microbial membrane (Fig. 1).

2. The higher antimicrobial activity of compounds **4, 11** and **12** may be due to the presence of electron withdrawing NO_2 group at *para* position of phenyl ring. Role of electron withdrawing group in improving antimicrobial activity is in accordance with the finding of Sharma *et al*. (2004).

3. Synthesized derivatives demonstrated low antibacterial and antifungal activity compared to reference drugs Ciprofloxacin and Fluconazole respectively, against all tested microbial species.

4. The presence of electron donating OCH_3 group (**5**, **8** and **12**) conferred higher antibacterial activity to the synthesized thiazole derivatives, specifically against *S. aureus* and *E.coli* (pMIC range = 4.49-4.60).

5. Compound (**6**) synthesized from cinnamic acid, has displayed better activity as compared to unsubstituted derivative (**2**). This may be due to the presence of extended conjugation in cinnamic acid, which may be involved in binding of synthesized compound with target site. This fact is supported by study of Narasimhan *et al*. (2007).

6. The aforementioned results indicated the fact that different structural requirements are essential for a compound to be selected as antibacterial or antifungal agent. This is similar to the results obtained by Sortino *et al*. (2007).

Molecular docking studies

Molecular docking studies were carried out to understand the binding profile of synthesized thiazole derivatives and to support the *in vitro* antimicrobial activity data. Automated docking was used to determine the orientation of inhibitors bound in the active site of bacterial glucosamine-6-phosphate synthase (PDB ID 1jxa) (Sarojini *et al.*, 2010). A Lamarckian genetic algorithm method, implemented in the program AutoDock Vina 1.1.2, was employed. The 3D-structure of bacterial glucosamine-6-phosphate synthase is presented in Fig. 2**.**

The docking of series of ligands (**2-12**) with glucosamine-6-phosphate synthase (GlcN-6-P synthase) indicated that all the synthesized compounds have potential of binding with one or the other amino acids in the active pockets as evident from the docking scores provided in Table 3. The 2D structure of ligand was drawn on ChemBioDrawUltra 12.0. and 3D coordinates were developed using ChemBio3D ultra 12.0 after performing MM2 minimization.

The protein structure file (PDB ID: 1jxa) taken from RCSB Protein Data Bank (PDB) was prepared for docking by removal of water molecules, adding polar hydrogens and Kollman charges to the structure file. *In silico* prediction of amino acids involved in the active site of protein responsible for binding with the ligands are obtained from the co-crystallized endogenous ligand from the PDB file. Ligand preparation is done by adding Gasteiger charges. Different conformations of ligands were built by allowing rotation of all torsions during docking.

Theoretically all the synthesized compounds showed very good binding scores ranging from -5.4 to -9.1 kcal/mol. Out of the ten compounds nine have shown docking scores much better than the docking score of co-crystallized ligand (-5.9 kcal/mol). Molecular docking studies revealed that compounds **11** and **12** is showing excellent binding score of more than -9.0 kcal/mol as the nitro group at *para* position in these compounds is making hydrogen bonding interaction with Arg383 and Arg173 (in **11**) and with Glu396 and Gln346 (in **12**) (Figure 3).

These compounds are also showing strong hydrophobic interaction with Pro177. In case of compound **12**, an extra π-stacking interaction which is generally known as sandwich type π-stacking interaction is being shown by Phe205 and Pro177 through the phenyl moiety carrying methoxy group. It can be justified as result of electron releasing effect of methoxy group which might increased the electron density of the π –cloud of the aromatic ring of the ligand and helps in providing sufficient stabilization.

Thus, hydrophobic interactions also tend to stabilize the binding site and thus should be considered as important parameter for drug design. The stabilization of receptor-ligand binding state through hydrophobic interactions is also reported by Singh *et al.* (2014) for biguanide based compounds for quorum sensing activity. The present data supports the *in vitro* results which suggest that compounds **11** and **12** are showing high antimicrobial activity against all the tested microorganisms. Hence, it can be predicted that activity may be due to inhibition of enzyme GlcN-6-P synthase, which catalyses a reaction which involves transfer of amine group from L-glutamine to Fru-6-P, followed by isomerisation of the fructosamine-6-phosphate to glucosamine-6-phosphate.

QSAR studies
Development of one-target QSAR models (ot-QSAR)

Quantitative structure activity relationship (QSAR) is one of the most influential method for the prediction of biological

activity of compounds. QSAR technique also important in finding quantitative relationships between the molecular structure and biological activity of investigated compounds (Mohsen *et al.*, 2010). In the present study, we have performed the QSAR studies by Hansch's analysis using the linear free energy relationship (LFER) model described by Hansch and Fujita (1964).

In Hansch's approach, structural properties of compounds are calculated in terms of different physicochemical parameters and these parameters are correlated with biological activity through equation using regression analysis. Before using the biological activity data for QSAR study experimentally determined MIC values changed to –log MIC or pMIC (in micromole) to get all the values positive, normal distribution of errors and to get linear free energy relationship of these data with physicochemical parameters. Further, regression analysis was performed using calculated physicochemical parameters (Table 4 and 5) as independent variables and antimicrobial activity values as dependent variables (Table 2).

On the basis of intercorrelation between the independent variables and also their individual correlation with antimicrobial activity, different probable combinations of parameters were subjected to linear regression (LR) and multiple linear regression (MLR) analysis. Out of hundreds of equations generated, some of the best QSAR equations having significant statistical values are selected.

These equations were generated in stepwise manner by forward selection method starting with best single variable and adding further significant variable according to their contribution to the model that leads to the smallest standard deviation (s), until there is no other variable outside the equation that satisfies the selection criteria.

The different physicochemical parameters *viz.* topological, electronic, thermodynamic, and spatial (Hansch and Fujita, 1964; Hansch *et al.*, 1973; Kier and Hall, 1976; Randic 1975; Balaban 1982; Wiener, 1947; Randic, 1993) were quantified using TSAR 3.3 software (TSAR 3D for Windows, Version 3.3, 2000) for synthesized thiazole derivatives are summarized in Table 4 and the values of selected parameters are presented in Table 5.

In view of above facts, a data set of 10 synthesized thiazole derivatives was used for model development. The predictive powers of derived QSAR models were confirmed by leave one out (LOO) method (Schaper, 1999), where a model is built with N - 1 compounds and N^{th} compound is predicted. Each compound is eliminated for model derivation and predicted in turn. The same procedure is repeated after elimination of another compound until all the compounds have been eliminated once.

A correlation matrix constructed for antibacterial activity against *S. aureus* is presented in Table 6. Both high and low colinearity was observed between different physicochemical properties. A highest interrelationship was observed between $^1\chi^v$ and MR (r = 0.997) and lowest interrelationship was observed between $^3\chi$ and log P (r = 0.376). The correlations of different parameters with antimicrobial activities are presented in Table 7.

A significant correlation (r > 0.7) was observed against all tested microbial strains with most of selected parameters except $^3\chi$ (Table 7).

ot-QSAR model for antibacterial activity against S. aureus

$pMIC_{sa} = 0.462\ (\pm 0.054)\ ^2\chi^v + 1.834\ (\pm 0.278)$ eq.1

n = 10   r = 0.950 r^2 = 0.902
q^2 = 0.891   s = 0.135 F = 74.361

$pMIC_{sa} = 1.039(\pm 0.195)\ ^2\chi^v - 0.468\ (\pm 0.156)\kappa_3 + 0.852(\pm 0.381)$ eq.2

n = 10   r = 0.979 r^2 = 0.958
q^2 = 0.946   s = 0.096 F = 79.084
PRESS = 0.064   RMSE = 0.253

The developed QSAR equation (Eq. 1) showed that the valence second order connectivity index ($^2\chi^v$) is favorable for antibacterial activity against *S. aureus*. The coefficient of $^2\chi^v$ is positive which indicated that activity against *S. aureus* increases with increase in $^2\chi^v$ value of synthesized thiazole derivatives. This is clearly evident from Table 5, that compounds (**4**, **8** and **12**) having high $^2\chi^v$ values, 5.59, 5.66 and 5.95 have high antibacterial activity values (Table 2), 4.51, 4.51 and 4.60, respectively. Similarly, compounds (**2** and **10**) with low $^2\chi^v$ values (3.40 and 3.84) have low antibacterial activity ($pMIC_{sa}$ = 3.39 and 3.59, respectively) against *S. aureus* (Table 2).

Although there is high interrelationship (r = 0.950, Eq. 1) between $^2\chi^v$ and other parameters, still we go for the development of biparametric models to get better regression coefficient. The maximum increase in r value was observed on combination of $^2\chi^v$ and Kier's shape topological index (κ_3) (r = 0.979, Eq. 2). High r (0.979) and q^2 (0.946) values revealed the significance of $^2\chi^v$ and κ_3 (Eq. 2) in describing antibacterial activity against *S. aureus* of synthesized thiazole derivatives.

The values of r and q^2 for Eq. 2 are 0.979 and 0.946, which means that the resulted QSAR model could explain and predict 97.9% and 94.6% of variances, respectively. Generally, when q^2 are larger than 0.5, the model are considered to have sound predictive power. However, several studies recommended that a high q^2 appear to be a necessary, but not sufficient, condition for a model to have a highly accurate predictive power (Oltulu *et al.*, 2009). Consequently, various other statistical approaches were used to validate the robustness and the practical applicability of the developed QSAR models.

To demonstrate that the resulted equations have good prediction of antimicrobial activity of selected thiazole derivatives, some different methods of evaluation of model performance have been used. Here, r^2, which presents the explained variance for given set, was used to determine the goodness of model's fit performance. Low values of RMSE and PRESS further confirmed the validity of developed QSAR models. Moreover, low residual values indicated that experimental and predicted antimicrobial activities are very close to each other also confirmed the robustness of developed models (Table 8).

Fig. 1: Structural requirements for antimicrobial activity of synthesized 2,4-disubstituted thiazole derivatives.
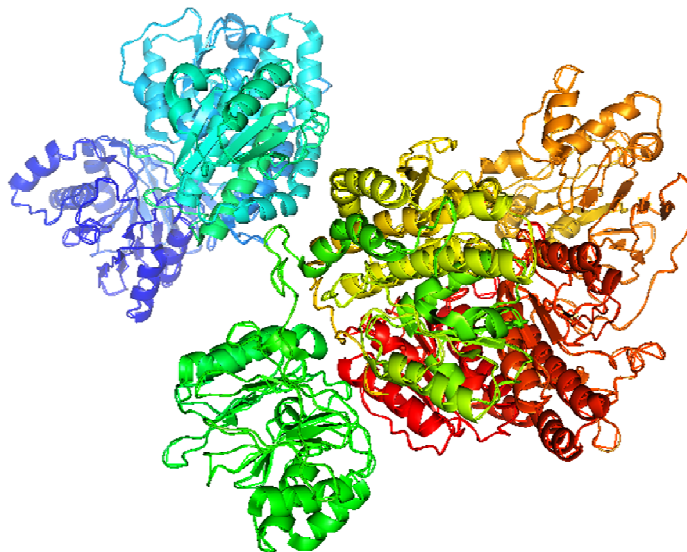
Fig. 2: Structure of bacterial glucosamine-6-phosphate synthase (PDB ID 1jxa).

11   **12**
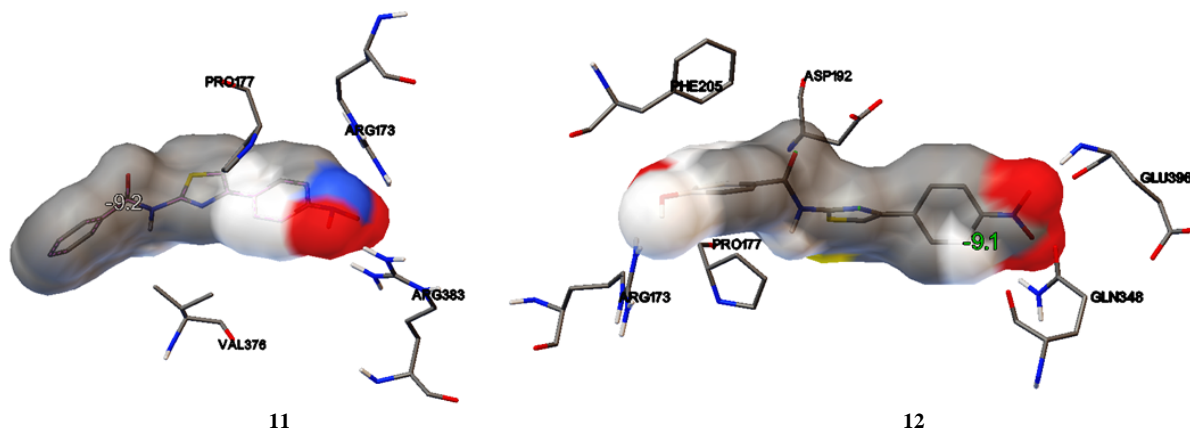
Fig. 3: The binding of ligands (**11** and **12**) on A chain amino acids present in an active site of GlcN-6-P with hydrogen bonds and hydrophobic interactions.

Table 1: Physicochemical properties of the synthesized thiazole derivatives

Compounds	Mol. Formula	Mol. Wt.	Mp (ºC)	R_f	% yield	R
2	$C_9H_8N_2S$	176	138-141	0.89[a]	78.2	-
3	$C_{16}H_{12}N_2OS$	280	98-101	0.85[c]	71.5	H
4	$C_{16}H_{11}N_3O_3S$	325	169-172	0.77[d]	73.2	NO_2
5	$C_{17}H_{14}N_2O_2S$	310	163-166	0.58[d]	67.7	OCH_3
6	$C_{18}H_{14}N_2OS$	306	174-177	0.78[d]	68.6	H
7	$C_{15}H_{11}N_3OS$	281	188-191	0.55[a]	55.1	-
8	$C_{18}H_{16}O_2N_2S$	324	224-227	0.65[b]	62.2	-
10	$C_9H_7O_2N_3S$	221	221-224	0.54[a]	55.4	-
11	$C_{16}H_{11}O_3N_3S$	325	203-206	0.73[a]	60.9	H
12	$C_{17}H_{13}O_4N_3S$	355	198-201	0.73[a]	46.1	OCH_3

TLC mobile phase – [a]Hexane : Ethyl acetate (1 : 2); [b]Pet. Ether : Ethyl acetate (7 : 1); [c]Hexane : Ethyl acetate (1 : 4); [d]Hexane : Ethyl acetate (2 : 1)

Table 2: pMIC values of synthesized 2,4-disubstituted thiazole derivatives

Comp.	Minimum inhibitory concentration (µM ml^{-1})							
	pMIC$_{bs}$	pMIC$_{sa}$	pMIC$_{ec}$	pMIC$_{ca}$	pMIC$_{an}$	pMIC$_{ab}$	pMIC$_{af}$	pMIC$_{am}$
2	3.39	3.39	3.39	3.39	3.39	3.39	3.39	3.39
3	3.79	4.41	4.41	3.79	3.79	4.20	3.79	4.04
4	3.93	4.51	4.51	3.93	3.93	4.32	3.93	4.16
5	3.89	4.49	4.49	3.89	3.89	4.29	3.89	4.13
6	3.87	4.18	4.18	3.57	3.87	4.08	3.72	3.94
7	3.20	4.11	4.11	3.81	3.81	3.80	3.81	3.80
8	3.92	4.51	4.51	3.92	3.92	4.31	3.92	4.16
10	3.59	3.59	3.59	3.29	3.59	3.59	3.44	3.53
11	3.93	4.23	4.23	3.93	4.23	4.13	4.08	4.11
12	4.01	4.60	4.60	4.01	4.01	4.40	4.01	4.24
S.D.	0.27	0.41	0.41	0.25	0.23	0.34	0.23	0.29
Std.*	2.61^a	2.61^a	2.61^a	2.64^b	2.64^b	2.61	2.64	2.62

S.D. Standard deviation ^{a} Ciprofloxacin ^{b} Fluconazole

Table 3: Docking score of synthesized thiazole derivatives against A chain amino acid present in active site of glucosamine-6-phosphate synthase.

Compound	Docking score (kcal/mol)
Co-crystallized ligand	-5.9
2	-5.4
3	-6.8
4	-7.3
5	-6.9
6	-6.7
7	-6.7
8	-8.1
10	-7.0
11	-9.2
12	-9.1

Table 4: Brief description of some molecular descriptors used in the present study

S. No.	Descriptor type	Molecular Description
1	Topological	Kier's molecular connectivity ($^0\chi$, $^0\chi^v$, $^1\chi$, $^1\chi^v$, $^2\chi$, $^2\chi^v$), Kier's alpha shape ($\kappa\alpha_1$) topological indices, Kier's shape (κ) topological indices, Randic topological index (R), Balaban topological index (J) and Wiener topological index (W)
2	Quantum	Total energy (Te), Ionization potential (I.P.), energies of highest occupied molecular orbital (HOMO) and lowest unoccupied molecular orbital (LUMO), dipole moment (μ) and electronic energy (Ele.E)
3	Lipophilic	Log P (Octanol-water partition coefficient)
4	Spatial	Molecular surface area , Molar volume (Vm)
5	Structural	Molecular Weight (MW)

Table 5: Value of selected descriptors used in the regression analysis

Comp.	Log P	$^0\chi$	$^1\chi$	$^2\chi$	$^2\chi^v$	$^3\chi$	$^3\chi^v$	κ^3	$\kappa\alpha_2$	$\kappa\alpha_3$	R	B
2	2.48	8.39	5.86	5.08	3.40	0.62	0.31	2.04	3.38	1.76	9.25	1.92
3	4.03	13.79	9.83	8.45	5.15	0.94	0.43	4.02	6.12	3.23	14.81	1.57
4	3.98	16.23	11.13	9.97	5.59	1.44	0.54	4.76	6.91	3.76	15.72	1.59
5	3.78	15.36	10.76	9.24	5.51	1.14	0.49	4.52	6.97	3.70	16.49	1.59
6	4.44	15.20	10.81	9.26	5.56	1.03	0.45	5.26	7.30	4.24	16.63	1.56
7	3.18	13.79	9.83	8.45	5.02	0.94	0.43	4.02	6.34	3.37	14.38	1.56
8	4.54	16.07	11.30	9.43	5.66	1.07	0.49	4.76	7.92	4.11	17.75	1.60
10	2.44	10.84	7.16	6.60	3.84	1.12	0.43	2.77	4.18	2.28	10.16	1.97
11	3.98	16.23	11.13	9.97	5.59	1.44	0.54	4.76	6.91	3.76	15.72	1.59
12	3.73	17.81	12.06	10.76	5.95	1.64	0.61	5.26	7.76	4.24	17.40	1.60

Table 6: Correlation matrix for antimicrobial activity of synthesized thiazole derivatives against *S. aureus.*

	Log P	MR	χ^0	$^0\chi^v$	$^1\chi$	$^1\chi^v$	$^2\chi$	$^2\chi^v$	$^3\chi$	$^3\chi^v$	κ_3	$\kappa\alpha_3$	SA
Log P	1												
MR	0.906	1											
χ^0	0.808	0.973	1										
$^0\chi^v$	0.873	0.995	0.980	1									
$^1\chi$	0.852	0.990	0.993	0.992	1								
$^1\chi^v$	0.897	0.997	0.969	0.992	0.991	1							
$^2\chi$	0.794	0.964	0.997	0.968	0.989	0.963	1						
$^2\chi^v$	0.876	0.994	0.984	0.991	0.997	0.997	0.981	1					
$^3\chi$	0.376	0.645	0.796	0.671	0.721	0.626	0.809	0.684	1				
$^3\chi^v$	0.557	0.808	0.917	0.837	0.865	0.795	0.919	0.836	0.963	1			
κ_3	0.874	0.984	0.966	0.968	0.978	0.978	0.965	0.981	0.681	0.815	1		
$\kappa\alpha_3$	0.884	0.990	0.959	0.979	0.976	0.982	0.950	0.978	0.634	0.789	0.992	1	
SA	0.832	0.937	0.930	0.950	0.945	0.948	0.921	0.950	0.630	0.797	0.887	0.890	1

ot-QSAR model for antibacterial activity against E. coli

$pMIC_{ec} = 0.462\ (\pm 0.054)\ ^2\chi^v + 1.834\ (\pm 0.278)$ eq.3

n = 10   r = 0.950 r^2 = 0.903 q^2 = 0.891

s = 0.135   F = 74.361

$pMIC_{ec} = 1.039(\pm 0.195)\ ^2\chi^v - 0.468(\pm 0.156)\kappa_3 + 0.852(\pm 0.381)$ eq.4

n = 10   r = 0.979 r^2 = 0.958

q^2 = 0.946   s = 0.096 F = 79.084

PRESS = 0.064   RMSE = 0.253

QSAR analysis of *E. coli* once again revealed the significance of $^2\chi^v$ and κ_3 in demonstrating antimicrobial activity. Further, developed QSAR model indicated that antimicrobial activity is positively correlated with $^2\chi^v$ and negatively correlated with κ_3 (Eq. 3 and Eq. 4).

ot-QSAR model for antibacterial activity against B. subtilis

$pMIC_{bs} = 2.50\ (\pm 0.772)\ ^3\chi^v + 2.575\ (\pm 0.368)$ eq.5

n = 10   r = 0.753 r^2 = 0.567 q^2 = 0.513 s = 0.188   F = 10.492

$pMIC_{bs} = 1.681\ (\pm 0.823)\ ^3\chi^v + 0.163\ (\pm 0.091)$ log P + 2.365 ($\pm$ 0.347)   Eq. 6

n = 10   r = 0.839 r^2 = 0.704 q^2 = 0.618

s = 0.166   F = 8.30

PRESS = 0.196   RMSE = 0.442

In case of *B. subtilis* the developed QSAR model (Eq. 5) showed that there is a positive correlation between antibacterial activity of synthesized thiazole derivatives and their $^3\chi^v$ values. This is supported by antibacterial activity values of synthesized thiazole derivatives (Table 2) and their $^3\chi^v$ values (Table 5). Further, during multiple linear regression (MLR) study there was a significant increment in r value on addition of log P to $^3\chi^v$. [r = 0.753 (Eq. 5) to r = 0.839 (Eq. 6)]. Topological indices parameters (e.g. $^1\chi$ and $^3\chi^v$) are numerical descriptors of a topology of a molecule. These are highly sensitive to bonding pattern, symmetry, content of heteroatom as well as degree of complexity of atomic neighborhoods. Since connectivity order of the constituent atoms in a molecule can be described by topological descriptors hence the information based upon connectivity can reveal the role of structural or sub-structural information of a molecule in estimating biological activity, *viz.* antimicrobial activity. Therefore, topological descriptors developed for predicting physicochemical properties and biological activities of chemical substance can be used for drug design (Lather and Madan, 2005).

ot-QSAR model for antifungal activity against C. albicans

$pMIC_{ca} = 0.258\ (\pm 0.050)\ ^2\chi^v + 2.432\ (\pm 0.262)$ eq.7

n = 10   r = 0.876

q^2 = 0.738   s = 0.127

F = 26.343

$pMIC_{ca} = 0.896(\pm 0.128)\ ^2\chi^v - 0.519(\pm 0.102)\ \kappa_3 + 1.345(\pm 0.250)$ eq.8

n = 10   r = 0.975

q^2 = 0.936   s = 0.063   F = 66.691

PRESS = 0.028   RMSE = 0.166

In case of *C. albicans* $^2\chi^v$ found to be the major factor influencing the antifungal activity (Eq. 7). Further, on combination of κ_3 with $^2\chi^v$, statistical more significant biparametric model was developed, as the value of r increased from 0.876 (Eq. 7) to 0.975 (Eq. 8). Hence Eq. 8 has more predictability than Eq. 7, which can also be observed from low residual values (Table 8). Consequently, the topological parameter $^2\chi^v$ as well Kier's shape topological parameter, κ_3 playing a significant role in determining the activity of thiazole derivatives against *C. albicans*.

ot-QSAR model for antifungal activity against A. niger

$pMIC_{an} = 0.123\ (\pm 0.018)\ ^2\chi + 2.770\ (\pm 0.162)$ eq.9

n = 12   r = 0.922

r^2 = 0.850 q^2 = 0.831

s = 0.093   F = 45.290

PRESS = 0.068   RMSE = 0.261

The developed QSAR equation (Eq. 9) for *A. niger* depicted that second order connectivity index ($^2\chi$) is positively correlated with antifungal activity of synthesized substituted thiazole derivatives. These results can be evidenced by high $^2\chi$ values (9.97 and 10.76, Table 5) of compounds **11** and **12** having highest antifungal activity ($pMIC_{an}$ = 4.23 and 4.01, Table 2) against *A. niger,* respectively.

The cross-validation of the developed models was performed by leave one out (LOO) method (Schaper, 1999). As per studies done by Golbraikh and Troposha for a valid QSAR model the value of cross validated r^2 (q^2) should be more than 0.5 (Golbraikh and Tropsha *et al.*, 2002). Consequentially, all the QSAR models developed in present study are statistically valid and reliable in predicting the antimicrobial activity of synthesized thiazole derivatives. The plot of observed $pMIC_{sa}$ Vs predicted $pMIC_{sa}$ (Fig. 4) showed the accuracy of developed *ot*-QSAR model (Eq. 2).
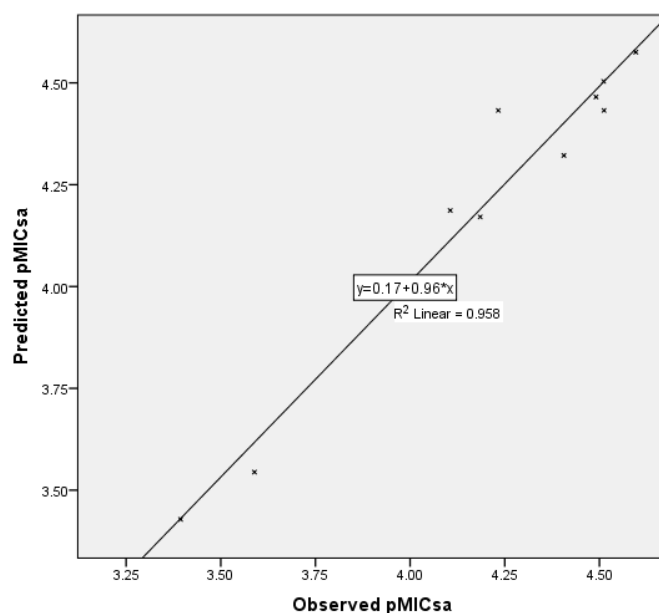
Fig. 4: Plot of observed $pMIC_{sa}$ values against predicted $pMIC_{sa}$ values for the multiple linear regression developed model by Eq. 2

Table 7: Correlation of molecular descriptors with antimicrobial activity of synthesized thiazole derivatives

Mol. Descriptor	pMIC$_{bs}$	pMIC$_{sa}$	pMIC$_{ec}$	pMIC$_{ca}$	pMIC$_{an}$	pMIC$_{ab}$	pMIC$_{af}$	pMIC$_{am}$
Log P	0.725	0.832	0.832	0.691	0.733	0.854	0.745	0.843
MR	0.722	0.937	0.937	0.844	0.867	0.937	0.896	0.950
$^{0}\chi$	0.739	0.930	0.930	0.874	0.912	0.936	0.935	0.962
$^{0}\chi^{v}$	0.717	0.950	0.950	0.876	0.866	0.946	0.913	0.962
$^{1}\chi$	0.707	0.945	0.945	0.882	0.900	0.939	0.934	0.963
$^{1}\chi^{v}$	0.689	0.948	0.948	0.868	0.867	0.937	0.909	0.954
$^{2}\chi$	0.727	0.921	0.921	0.870	0.922	0.925	0.938	0.955
$^{2}\chi^{v}$	0.714	0.950	0.950	0.876	0.889	0.945	0.925	0.965
$^{3}\chi$	0.696	0.630	0.630	0.632	0.775	0.684	0.734	0.719
$^{3}\chi^{v}$	0.753	0.797	0.797	0.783	0.853	0.833	0.856	0.863
κ_1	0.743	0.929	0.929	0.866	0.907	0.935	0.929	0.959
κ_2	0.707	0.930	0.930	0.842	0.875	0.927	0.899	0.944
κ_3	0.714	0.887	0.887	0.776	0.868	0.895	0.860	0.908
$\kappa\alpha_1$	0.728	0.930	0.930	0.871	0.893	0.933	0.924	0.956
$\kappa\alpha_2$	0.674	0.925	0.925	0.839	0.845	0.915	0.883	0.930
$\kappa\alpha_3$	0.686	0.890	0.890	0.780	0.843	0.890	0.850	0.901
R	0.698	0.941	0.941	0.847	0.826	0.934	0.877	0.942
B	-0.438	-0.870	-0.870	-0.840	-0.773	-0.809	-0.847	-0.843
W	0.725	0.903	0.903	0.802	0.765	0.910	0.822	0.908

Table 8: Comparison of observed and predicted antibacterial and antifungal activity obtained by *ot*-QSAR models

Comp.	pMIC$_{sa}$ MLR (Eq. 2)			pMIC$_{ec}$ MLR (Eq. 4)			pMIC$_{bs}$ MLR (Eq. 6)			pMIC$_{ca}$ MLR (Eq. 8)			pMIC$_{an}$ (Eq. 9)		
	Obs.	Pre.	Res.	Obs.	Pre.	Res.	Obs.	Pre.	Res.	Obs.	Pre.	Res.	Obs.	Pre.	Res.
2	3.43	3.39	-0.03	3.43	3.39	-0.03	3.29	3.39	0.10	3.33	3.39	0.06	3.39	3.39	0.00
3	4.32	4.41	0.08	4.32	4.41	0.08	3.74	3.79	0.05	3.87	3.79	-0.08	3.81	3.79	-0.02
4	4.43	4.51	0.08	4.43	4.51	0.08	3.92	3.93	0.01	3.88	3.93	0.05	4.00	3.93	-0.07
5	4.47	4.49	0.03	4.47	4.49	0.03	3.80	3.89	0.09	3.94	3.89	-0.05	3.91	3.89	-0.02
6	4.17	4.18	0.01	4.17	4.18	0.01	3.85	3.87	0.02	3.60	3.57	-0.03	3.91	3.87	-0.04
7	4.19	4.11	-0.08	4.19	4.11	-0.08	3.61	3.20	-0.41	3.76	3.81	0.05	3.81	3.81	0.00
8	4.50	4.51	0.01	4.50	4.51	0.01	3.93	3.92	-0.01	3.94	3.92	-0.03	3.93	3.92	-0.01
10	3.54	3.59	0.04	3.54	3.59	0.04	3.49	3.59	0.10	3.35	3.29	-0.06	3.58	3.59	0.01
11	4.43	4.23	-0.20	4.43	4.23	-0.20	3.92	3.93	0.01	3.88	3.93	0.05	4.00	4.23	0.23
12	4.58	4.60	0.02	4.58	4.60	0.02	4.00	4.01	0.01	3.95	4.01	0.06	4.09	4.01	-0.08

**Table 9:** Comparison of observed and predicted antimicrobial activity obtained by *mt*-QSAR models.

Comp.	pMIC$_{ab}$ (Eq. 10)			pMIC$_{af}$ MLR (Eq. 12)			pMIC$_{am}$ MLR (Eq. 13)		
	Obs.	Pre.	Res.	Obs.	Pre.	Res.	Obs.	Pre.	Res.
2	3.38	3.39	0.02	3.34	3.39	0.05	3.39	3.39	0.01
3	4.02	4.20	0.18	3.77	3.79	0.03	4.04	4.04	0.00
4	4.24	4.32	0.08	3.98	3.93	-0.05	4.14	4.16	0.02
5	4.18	4.29	0.12	3.86	3.89	0.03	4.11	4.13	0.02
6	4.18	4.08	-0.10	3.76	3.72	-0.03	3.97	3.94	-0.03
7	4.02	3.80	-0.22	3.77	3.81	0.04	3.90	3.80	-0.10
8	4.26	4.31	0.05	3.86	3.92	0.05	4.07	4.16	0.09
10	3.59	3.59	0.00	3.56	3.44	-0.12	3.50	3.53	0.03
11	4.24	4.13	-0.10	3.98	4.08	0.10	4.14	4.11	-0.03
12	4.39	4.40	0.01	4.07	4.01	-0.07	4.22	4.24	0.02

To examine the presence of a systemic error in developed QSAR equation (Eq. 2), the observed pMIC$_{sa}$ values were plotted against the residuals pMIC$_{sa}$ values (Fig. 5). The presence of the residual points on both sides of zero indicated that no systemic error exists in the development of QSAR model. (Golbraikh and Tropsha *et al.*, 2002). Usually for QSAR analysis, the biological activity data of synthesized molecules should lies in between 2–3 orders of magnitude. Although, in present study the range of anti-microbial activities of synthesized thiazole derivatives is within one order of magnitude, though the low residual values (Table 8) evidenced the high predictability of developed QSAR models (Eqs. 1-9). This is in agreement with results suggested by earlier studies (Narasimhan *et al.*, 2007; Sharma *et al.*, 2006; Hatya *et al.*,

2006; Kumar *et al.*, 2006), which confirmed that the robustness of the QSAR model lies in its predictive ability, although the biological activity data existed in narrow range of magnitude. Moreover, Kim *et al.* (2007) recommended that developed QSAR models are acceptable if the value of standard deviation is not much higher than 0.3. Hence, the above facts justify the statistical acceptability of developed QSAR models (Eqs. 1-9).

Development of multi-target QSAR model (mt-QSAR)

Aforementioned *ot*-QSAR models showed that five different equations have to be used to predict the activity of synthesized derivatives against the respective bacterial and fungal strains. But results of our earlier studies recommended that use of
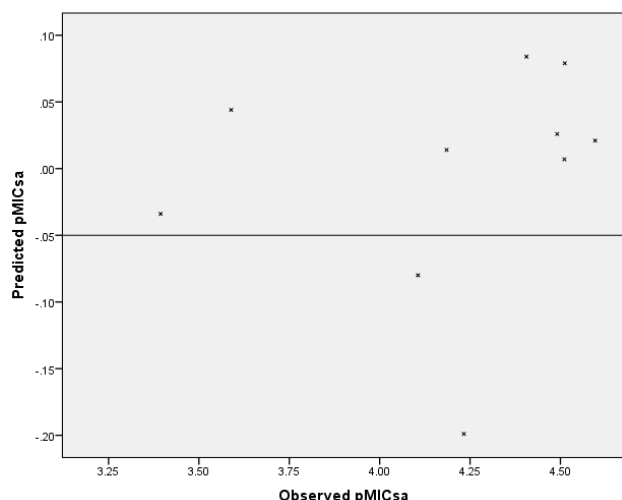
Fig. 5: Plot of observed $pMIC_{sa}$ values against residual $pMIC_{sa}$ values for the multiple linear regression developed model by Eq. 2

ot-QSAR equations is not much practicable, when we have to predict the activity of synthesized compounds against more than one target. As different *ot*-QSAR equations have to be used for different targets. Above facts inspired us to develop multi-target QSAR (*mt*- QSAR) models. In contrast to *ot*-QSAR, the *mt*-QSAR model is a single equation that considers common and essential physicochemical parameters for describing the antimicrobial activity for different targets (Prado -Prado *et al.*, 2008; Gonzalez-Diaz *et al.*, 2007, 2008a; Gonzalez-Diaz and Prado-Prado 2008; Cruz-Monteagudo *et al.*, 2007).

In the present study we have attempted to develop three different types of *mt*-QSAR models *viz. mt*-QSAR model for describing antibacterial activity of synthesized compounds against *S. aureus, B. subtilis* and *E. coli, mt*-QSAR model for describing antifungal activity of synthesized compounds against *C. albicans* and *A. niger* as well a common *mt*-QSAR model for describing the antimicrobial (overall antibacterial and antifungal) activity of synthesized thiazole derivatives against all the above mentioned microorganisms. In order to build up *mt*-QSAR equations, firstly we have calculated the average antibacterial, antifungal and antimicrobial activities values of synthesized thiazole derivatives which are presented in Table 2. Further, these average antimicrobial activity values were interrelated with the physicochemical parameters (Table 5) of synthesized compounds.

mt-QSAR model for antibacterial activity

$pMIC_{ab} = 0.163\ (\pm 0.021)\ ^1\chi + 2.422\ (\pm 0.214)$ Eq. 10

n = 12	r = 0.938	$r^2 = 0.880$	$q^2 = 0.868$
s = 0.125	F = 59.934		
PRESS = 0.124	RMSE = 0.352		

In case of *mt*-QSAR model for antibacterial activity revealed the significance of first order molecular connectivity index ($^1\chi$) in describing antibacterial activity of synthesized thiazole derivatives. Positive coefficient of $^1\chi$ in developed model (Eq. 10) implies that antibacterial activity is directly proportional to value of $^1\chi$. This can be proved by high antibacterial values of

compounds **4**, **8** and **12** ($pMIC_{ab}$ = 4.32, 4.31 and 4.40, respectively) having high values of $^1\chi$ i.e. 11.13, 11.30 and 12.06 (Table 5), respectively.

mt-QSAR model for antifungal activity

$pMIC_{af} = 0.124\ (\pm 0.160)\ ^2\chi + 2.713\ (\pm 0.144)$ eq11

n = 12	r = 0.938	$r^2 = 0.880$	$q^2 = 0.865$
s = 0.083	F = 58.803		

$pMIC_{af} = 0.210(\pm 0.057)^2\chi - 0.144(\pm 0.092)\kappa_3 + 2.570(\pm 0.161)$ eq. 12

n = 12	r = 0.954	$r^2 = 0.910$	$q^2 = 0.885$
s = 0.076	F = 35.79		
PRESS = 0.041	RMSE = 0.203		

In case of *mt*-QSAR model for antifungal activity second order molecular connectivity index ($^2\chi$) was found to significant (Eq. 11). Once again the positive coefficient of molecular connectivity index directly correlates with antifungal activity. Further, as we go for development of biparametric models the combination $^2\chi$ and κ_3 produced statistically more significant equation (Eq. 12) which led to small increase in values of r [0.938, Eq. (11) to 0.954, Eq. (12)] and q^2 [0.865, Eq. (11) to 0.885, Eq. (12)] and lowering in value of standard deviation [0.083, Eq. (11) to 0.076, Eq. (12)].

mt-QSAR model for antibacterial activity

$pMIC_{am} = 0.654(\pm 0.105)\ ^2\chi^v - 0.337(\pm 0.106)\kappa\alpha_3 + 1.756(\pm 0.195)$ eq13

n = 12	r = 0.986	$r^2 = 0.972$	$q^2 = 0.963$
s = 0.055	F = 119.646		
PRESS = 0.022	RMSE = 0.145		

Further, in case of *mt*-QSAR model for overall antimicrobial activity when we go for development of biparametric model, statistically most significant and predictable equation was obtained by combining $\kappa\alpha_3$ and $^2\chi^v$ (Eq. 13) , which can be confirmed by low residual values (Table 9). Moreover, the developed model predicts 96.3% and explains 98.6% variances of antimicrobial activity.

The plot of observed $pMIC_{am}$ Vs predicted $pMIC_{am}$ (Fig. 6) showed the accuracy of developed *mt*-QSAR model (Eq. 13). Additionally there is no systemic error in developed model (Eq. 13), which can be confirmed by plot of residual $pMIC_{am}$ Vs observed $pMIC_{am}$ (Fig. 7) as the residual error values are present on both side of zero. Moreover, the small residual values of all tested bacterial and fungal strains presented in Table 8 and 9 were in concurrence with model expressed by Eq. 2, 4, 6, 8, 9, 10, 12 and 13. From the aforementioned QSAR models, it can be concluded that the molecular connectivity index and Kier's shape index, are key parameters for the antimicrobial activity of synthesized thiazole derivatives and can be cosidered as important factors for interaction with target site of different microorganisms. Moreover, *mt*-QSAR models found be statistically more significant in describing antimicrobial activity of synthesized thiazole derivatives than *ot*-QSAR models.
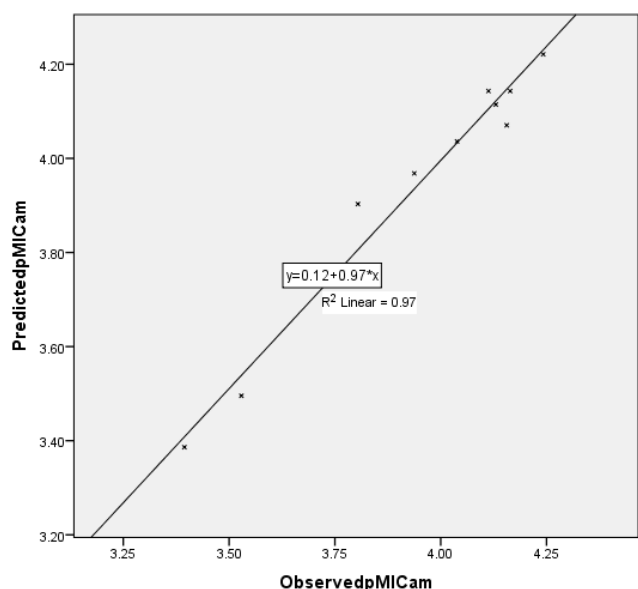
Fig. 6: Plot of predicted pMIC$_{am}$ values against observed pMIC$_{am}$ values for the MLR developed model by Eq. 13
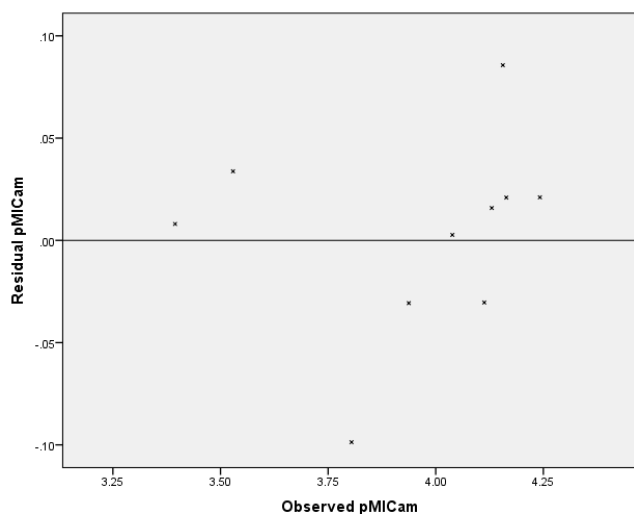

Fig. 7: Plot of residual pMIC$_{am}$ values against residual pMIC$_{am}$ values for the MLR developed model by Eq. 13.

CONCLUSION

In present study, *N*-(4-phenyl-thiazol-2-yl)-benzamide/amide derivatives (**3-7**, **9** and **11-12**) and (3,4-dimethoxy-benzylidene)-(4-phenyl-thiazol-2-yl)-amine (**8**) have been synthesized (Scheme 1 and 2) successfully in appreciable yields and evaluated for their *in vitro* antibacterial and antifungal activities against *B. subtilis, E. coli, S. aureus, C. albicans* and *A. niger* by tube dilution method. Chemical structures of synthesized compounds were ascertained on the basis of their spectral data (IR and ^{1}H NMR). The analysis of antimicrobial activity results indicated that the presence of NO$_2$ and OCH$_3$ groups at *para* position of phenyl ring improved the antimicrobial activity of the synthesized thiazole derivatives. The replacement of NH$_2$ group (**2**) with substituted phenyl ring (**3-8** and **11-12**) led to a noticeable increase in antimicrobial activity of the synthesized compounds against *S. aureus* and *E. coli*. Molecular docking studies revealed

that compounds **11** and **12** is showing excellent binding score of -9.2 kcal/mol and -9.1 kcal/mol, respectively as the nitro head group at *para* position is making strong hydrogen bonding interaction with Arg383, Arg173, Glu396 and Gln346 amino acid residues. These compounds also have potential to show sandwich type π-stacking interactions. Further, QSAR studies indicated that the molecular connectivity index ($^2\chi^v$) and Kier's shape index (κα$_3$) are key parameters for the antimicrobial activity of synthesized thiazole derivatives. The developed QSAR equations satisfy the statistical validation criteria to a considerable extent and can be a valuable theoretical base for proposing more potent 2,4-disubstituted thiazole derivatives.

REFERENCES

Balaban AT. Highly discriminating distance based topological indices. Chem Phys Lett, 1982; 89:399-404.

Ban M, Taguchi H, Katsushima T, Takahashi M, Shinoda K, Watanabe A, Tominaga T. Novel antiallergic and antiinflammatory agents. Part I: Synthesis and pharmacology of glycolic amide derivatives. Bioorg Med Chem, 1998; 6:1069-1076.

Bates CJ, Adams WR, Handschumacher RE. Control of the formation of uridine diphospho-*N*-acetyl-hexosamine and glycoprotein synthesis in rat liver. J Biol Chem, 1966; 241:1705-1712.

Bharti SK, Nath G, Tilak R, Singh SK. Synthesis, anti-bacterial and anti-fungal activities of some novel Schiff bases containing 2,4-disubstituted thiazole ring. Eur J Med Chem, 2010; 42:651-660.

Cappucino JG, Sherman N, 1999, Microbiology-a laboratory manual, Addison Wesley Longman Inc, California, 263.

Chmara H, Andruszkiewicz R, Borowski E, Inactivation of glucosamine-6-phosphate synthetase from *Salmonella typhimurium* LT 2 SL 1027 by N beta-fumarylcarboxyamido-L-2,3-diamino-propionic acid. Biochem Biophys Res Commun, 1984; 120:865-872.

Chmara H, Andruszkiewicz R, Borowski E. Inactivation of glucosamine-6-phosphate synthetase from Salmonella typhimurium LT2 by fumaroyl diaminopropanoic acid derivatives, a novel group of glutamine analogs. Biochim Biophys Acta, 1986; 870:357-366.

Cohen A, Verhaeghe P, Crozet MD, Hutter S, Rathelot P, Vanelle P, Azas N Tandem synthesis and *in vitro* antiplasmodial evaluation of new naphtho[2,1-d] thiazole derivatives Eur J Med Chem, 2012; 55:315-324.

Cruz-Monteagudo M, Gonzalez-Diaz H, Aguero-Chapin G, Santana L, Borges F, Dominguez ER, Podda G, Uriarte E. Computational chemistry development of a unified free energy Markov model for the distribution of 1300 chemicals to 38 different environmental or biological systems. J Comput Chem, 2007; 28(11):1909-1923.

Dutka-Malen S, Mazodier P, Badet B. Molecular cloning and overexpression of the glucosamine synthetase gene from *Escherichia coli*. Biochimie, 1988; 70:287-290.

El-Sabbagh OI, Baraka MM, Ibrahim SM, Pannecouque C, Andrei G, Snoeck R, Balzarini J, Rashad AA. Synthesis and antiviral activity of new pyrazole and thiazole derivatives. Eur J Med Chem, 2009; 44: 3746-3753.

Golbraikh A, Tropsha A. Beware of q^2!. J Mol Graphics Model, 2002; 20(4):269–276.

Gonzalez-Diaz H, Gonzalez-Diaz Y, Santana L, Ubeira FM, Uriarte E. Networks and connectivity indices. Proteomics, 2008a; 8(4): 750-778.

Gonzalez-Diaz H, Prado-Prado FJ. Unified QSAR and network-based computational chemistry approach to antimicrobials, part 1: Multi species activity models for antifungals. J Comput Chem, 2008; 29(4):656-667.

Gonzalez-Diaz H, Vilar S, Santana L, Uriarte E. Medicinal chemistry and bioinformatics-current trends in drugs discovery with networks topological indices. Curr Top Med Chem, 2007; 7(10):1015-1029.

Hansch C, Fujita T. p-σ-π Analysis. A method for the correlation of biological activity and chemical structure. J Am Chem Soc, 1964; 86:1616-1626.

Hansch C, Leo A, Unger SH, Kim KH, Nikaitani D, Lien EJ. Aromatic substituent constants for structure- activity correlations. J Med Chem, 1973; 16:1207-1216.

Hatya SA, Aki-Sener E, Tekiner-Gulbas B, Yildiz I, Temiz-Arpaci O, Yalcin I, Altanlar N. Synthesis, antimicrobial activity and QSARs of new benzoxazine-3-ones. Eur J Med Chem, 2006; 41:1398-1404.

Helal MHM, Salem MA, El-Gaby MSA, Aljahdali M. Synthesis and biological evaluation of some novel thiazole compounds as potential anti-inflammatory agents Eur J Med Chem, 2013; 65:517-526.

Hyperchem 6.0, Hypercube, Inc., Gainesville, 1993.

Jain A, Pandey V, Ganeshpurkar A, Dubey N, Bansal D. Formulation and characterization of floating microballoons of Nizatidine for effective treatment of gastric ulcers in murine model. Drug Deliv, 2014 DOI:10.3109/10717544.2014.891273.

Kier LB, Hall LH. 1976, Molecular connectivity in chemistry and drug research, New York: Academic Press, 79-82.

Kim Y, Farrah S, Baney RH. Structure–antimicrobial activity relationship for silanols, a new class of disinfectants, compared with alcohols and phenols. Int J Antimicrob Ag, 2007; 29:217–222.

Kumar A, Sharma P, Gurram VK, Rane N. Studies on synthesis and evaluation of quantitative structure–activity relationship of phosphorus10-methyl-6-oxo-5-arylazo-6,7-dihydro-5*H* (1,3) azapsholo (1,5-d) (1,4) benzodiazepin-2-phospha-3-ethoxycarbonyl-1-phosphorus dichlorides. Bioorg Med Chem Lett, 2006; 16:2484-2491.

Kumar D, Judge V, Narang R, Sangwan S, Clerq E. De, Balzarini J, Narasimhan B. Benzylidene/2-chlorobenzylidene hydrazides: Synthesis, antimicrobial activity, QSAR studies and antiviral evaluation. Eur J Med Chem, 2010; 45:2806-2816.

Kumar P, Narasimhan B, Sharma D, Judge V, Narang R. Hansch analysis of substituted benzoic acid benzylidene/furan-2-ylmethylene, hydrazides as antimicrobial agents. Eur J Med Chem, 2009; 44: 1853-1863.

Lather V, Madan AK. Topological models for the prediction of anti-HIV activity of dihydro (alkylthio) (naphthylmethyl) oxopyrimidines. Bioorg Med Chem, 2005, 13:1599-1604.

Milewski S, Chmara H, Andruszkiewicz R, Borowski E, Zaremba M, Borowski. Antifungal peptides with novel specific inhibitors of glucosamine 6-phosphate synthase. Drugs Exp Clin Res, 1988; 14:461-465.

Mjambili F, Njoroge M, Naran K, Kock CD, Smith PJ, Mizrahi V, Warner D, Chibale K. Synthesis and biological evaluation of 2-aminothiazole derivatives as antimycobacterial and antiplasmodial agents Bioorg Med Chem Lett, 2014; 24:560-564

Mohsen S, Razieh S, Maryam BZ, Behzad MF, Reza AK. QSAR study of anthranilic acid sulfonamides as inhibitors of methionine aminopeptidase-2 using LS-SVM and GRNN based on principal components. Eur J Med Chem, 2010; 45:4499-4508.

Narang R, Narasimhan B, Sharma S, (Naphthalen-1-yloxy)-acetic acid benzylidene/(1-phenyl-ethylidene)-hydrazide derivatives: Synthesis, antimicrobial evaluation and QSAR studies. Med Chem Res, 2012; 21:2526-2547.

Narang R, Narasimhan B, Sharma S, Sriram D, Yogeeswari P, Clercq ED, Balzarini J, Nicotinic acid benzylidene hydrazides: Synthesis, antitubercular, antiviral, antimicrobial evaluation and QSAR studies. Med Chem Res, 2012; 21:1557-1576.

Narang R, Narasimhan B, Sharma S, Sriram D, Yogeeswari P, Clercq ED, Balzarini J, Nicotinic acid benzylidene/phenyl-ethylidene hydrazides: Synthesis, antitubercular, antiviral, antimicrobial evaluation and QSAR studies. Lett Drug Design and Discov, 2011; 8:733-749.

Narang R, Narasimhan B, Sharma S, Sriram D., Yogeeswari P, Clercq ED, Balzarini J, Substituted naphthalen-1-yl-acetic acid benzylidene/(1-phenyl-ethylidene)-hydrazides: synthesis, antiviral, antibacterial and antifungal evaluation and QSAR analysis. Med Chem, 2013; 9:249-74.

Narasimhan B, Judge V, Narang R, Ohlan S, Ohlan R. Quantitative structure activity relationship studies for prediction of antimicrobial activity of synthesized 2,4-hexadienoic acid derivatives. Bioorg Med Chem Lett, 2007; 21:5836-5845.

Narasimhan B, Ohlan S, Ohlan R, Judge V, Narang R. Hansch analysis of veratric acid derivatives as antimicrobial agents. Eur J Med Chem, 2009; 44:689-700.

Nishikaku F, Koga Y, Suppression of murine collagen-induced arthritis by treatment with a novel thiazole derivative, SM-8849. Immunopharmacology, 1993; 25:65-74.

Novakova I, Subileau EA, Toegel S, Gruber D, Lachmann B, Urban E, Chesne C, Noe CR, Neuhaus W. Transport rankings of non-steroidal antiinflammatory drugs across blood-brain barrier *in vitro* models. PLoS One, 2014; 9:e86806.

Oltulu O, Yasar MM, Eroglu EA. QSAR study on relationship between structure of sulfonamides and their carbonic anhydrase inhibitory activity using the eigenvalue (EVA) method. Eur J Med Chem, 2009; 44:3439-344.

Ozdemir A, Turan-Zitouni G, Kaplancikli ZA, Revial G, Güven K. Synthesis and antimicrobial activity of 1-(4-aryl-2-thiazolyl)-3-(2-thienyl)-5-aryl-2-pyrazoline derivatives. Eur J Med. Chem 2007; 42:403-409.

Perez KK, Olsen RJ, Musick WL, Cernoch PL, Davis JR, Peterson LE, Musser JM. Integrating rapid diagnostics and antimicrobial stewardship improves outcomes in patients with antibiotic resistant Gram-negative bacteremia. J Infect, 2014; 69:216-225.

Pharmacopoeia of India, Controller of Publications, Ministry of Health Department, Govt. of India, New Delhi, 2007; I:37.

Popsavin M, Torovic L, Svircev M, Kojic V, Bogdanovic G, Popsavin V. Synthesis and antiproliferative activity of two new tiazofurin analogues with 2'-amido functionalities. Bioorg Med Chem Lett, 2006; 16:2773–2776.

Prado-Prado FJ, Gonzalez-Diaz H, de la Vega OM, Ubeira FM, Chou KC. Unified QSAR approach to antimicrobials. Part 3: First multi-tasking QSAR model for Input-Coded prediction, structural back-projection, and complex networks clustering of antiprotozoal compounds. Bioorgan Med Chem, 2008; 16(11):5871-5880.

Rahmutulla B, Matsushita K, Satoh M, Seimiya M, Tsuchida S, Kubo S, Shimada H, Ohtsuka M, Miyazaki M, Nomura F. Alternative splicing of FBP-interacting repressor coordinates c-Myc, P27Kip1/cyclinE and Ku86/XRCC5 expression as a molecular sensor for bleomycin-induced DNA damage pathway. Oncotarget, 2014; 15:2404-2417.

Randic M. Comparative Regression Analysis-Regressions Based on Single Descriptor. Croat Chem Acta, 1993; 66:289-312.

Randic M. On the Characterization of Molecular Branching. J Am Chem Soc, 1975; 97:6609-6615.

Sarojini BK, Krishna BG, Darshanraj CG, Bharath BR, Manjunatha H. Synthesis, characterization, *in vitro* and molecular docking studies of new 2,5-dichloro thienyl substituted thiazole derivatives for antimicrobial properties. Eur J Med Chem, 2010; 45:3490-3496.

Schaper KJ. Free-Wilson-type analysis of non-additive substituent effects on THPB dopamine receptor affinity using artificial neural networks. Quant Struct Act Relat, 1999; 18:354-360

Sevrioukova IF, Poulos TL. Dissecting cytochrome P450 3A4-ligand interactions using ritonavir analogues. Biochemistry, 2013;52: 4474-4481.

Sharma P, Kumar A, Sharma M. Synthesis and QSAR studies on 5-(2-(2-methylprop-1-enyl)-1*H*-benzimidazol-1yl)-4,6-diphenyl-pyrimidin-2-(5*H*)- thione derivatives as antibacterial. Eur J Med Chem, 2006; 41:833-840.

Sharma P, Rane N, Gurram VK. Synthesis and QSAR studies of pyrimido(4,5-d)pyrimidine-2,5-dione derivatives as potential antimicrobial agents. Bioorg Med Chem Lett, 2004; 14:4185-4190.

Shoichet BK, McGovern SL, Wei B, Irwin JJ. Lead discovery using molecular docking, Curr Opin Chem Bio, 2002; 6(4): 439–446.

Singh S, Wanjari PJ, Bhatia S, Sonwane VC, Chakraborti AK, Bharatam PV. Design, synthesis, biological evaluation and toxicity studies of *N, N*-disubstituted biguanides as quorum sensing inhibitors. Med Chem Res, 2014. DOI 10.1007/s00044-014-1255-y.

Soares MI, Brito AF, Laranjo M, Paixao JA, Botelho MF, Melo TMVDP. Chiral 6,7-bis(hydroxymethyl)-1*H*,3*H*-pyrrolo[1,2-c]thiazoles with anti-breast cancer properties. Eur J Med Chem, 2013; 60:254-262.

Sortino M, Delgado P, Jaurez S, Quiroga J, Abonia R, Insuasey B, Nogueras M, Rodero, L. Synthesis and antifungal activity of (Z)-5-arylidenerhodanines. Bioorg Med Chem Lett, 2007; 15:484-494.

SPSS for Windows, version 10.05, SPSS Inc., Bangalore, India 1999.

Styrt B, Rocklin RE, Klempner MS. Inhibition of neutrophil superoxide production by fanetizole. Inflammation. 1985; 9:233-244.

Trott O, Olson AJ. AutoDock Vina: improving the speed and accuracy of docking with a new scoring function, efficient optimization and multithreading, J Comput Chem, 2010; 31:455-461.

TSAR 3D Version 3.3, Oxford Molecular Limited, 2000.

Wei L, Cheng J, Meng Y, Ren Y, Deng H, Guo Y. A novel formulation of thiamine dilaurylsulphate and its preservative effect on apple juice and sterilised milk. Food Chem, 2014; 1:415-422.

Wiener H. Structural determination of paraffin boiling points. J Am Chem Soc, 1947; 69:17-20.

Ye J, Liu Q, Wang C, Meng Q, Sun H, Peng J, Ma X, Liu K. Benzylpenicillin inhibits the renal excretion of acyclovir by OAT1 and OAT3. Pharmacol Rep, 2013; 65:505-512.

Zablotskaya A, Segal I, Geronikaki A, Tatiana E, Belyakov S, Petrova M, Shestakova I, Zvejniece L, Nikolajeva V. Synthesis, physicochemical characterization, cytotoxicity, antimicrobial, anti-inflammatory and psychotropic activity of new N-[1,3-(benzo)thiazol-2-yl]-ω-[3,4-dihydroisoquinolin-2(1*H*)-yl]alkanamides. Eur J Med Chem, 2013; 70:846-856.